Int. J. Solids Structures Vol. 15, pp. 1–13
© Pergamon Press Ltd., 1979. Printed in Great Britain

0020-7683/79/0101-0001/$02.00/0

EXPERIMENTS ON DYNAMIC PLASTIC LOADING OF FRAMES†

S. R. BODNER‡ and P. S. SYMONDS§

Division of Engineering, Brown University, Providence, RI 02912, U.S.A.

(*Received* 27 *December* 1977; *in revised form* 5 *June* 1978)

Abstract—Tests are described on plane frames of mild steel and titanium (commercial purity) in which high intensity short duration pressure pulses were applied transversely to the beam member either uniformly over this member or concentrated at its center. The objective was to examine applications of two estimation techniques (upper bounds on deflections and the mode approximation technique) for major response features of pulse loaded structures at large deflections, taking account of strong plastic strain rate sensitivity. Loads over a range such as to cause final deflections up to about a third of the span were applied by detonating explosive sheet. Agreement between estimated and measured final deflections was often very good (generally conservative) but the intrinsic error of the mode technique was not observed as expected.

1. INTRODUCTION

The tests described here were part of a research program on estimation techniques for structures subjected to pulse loading such that large plastic deformations occur. In particular, extensions of deflection bound theorems and of the "mode approximation" technique to large deflections and viscoplastic material behavior are being investigated. The present tests were on structures in which large deflections do not drastically change the stiffness, the response remaining mainly flexural. In the same program, tests on fully clamped plates[2] were made, where the greatly increased stiffness at large deflections contrasts with the slightly decreased stiffness in the present frames.

The tests were designed to study the overall accuracy of the two estimation techniques. The deflection bounds and the deflection and response time estimates furnished by the mode technique involve two kinds of errors, "intrinsic" errors and further errors due to idealizations and approximations not essential to the method. In the present tests we hoped to assess their relative importance. The "idealizations and approximations" are almost all regarded as conservative, i.e. leading to deflection magnitudes larger than those expected in tests. These are discussed further in the concluding section. Full details of the present applications of the estimation techniques are given in a companion paper[1].

The intrinsic error in the deflection bound technique is, of course, positive, i.e. the computed deflection is an upper bound. That in the mode method arises from the device used for determining the amplitude of the initial mode form field from the specified initial velocity distribution. This error is negative if the specified initial velocity field is "more concentrated" than the mode shape, positive otherwise. In order to compare these, we used two types of loading, one with a concentrated impulse, the other with a uniformly distributed impulse. For each loading type, a range of impulse intensities was applied, giving final deflections up to about a third of the span, the basic measurements being the impulse, final deflected shape, and strain-time histories at several points. This program was carried out for frames for mild steel and commercial purity titanium, both having strongly rate sensitive plastic behavior. Parameters characterizing the material behavior were established by separate tests.

†Research supported by National Science Foundation under grant ENG74-21258 and by Office of Naval Research under Contract N00014-75-C-0860.

‡Visiting Professor of Engineering, Brown University, January–August 1976; on leave from Technion—Israel Institute of Technology, Haifa, Israel.

§Professor of Engineering, Brown University.

2. TEST TECHNIQUES

The two frames and loading types are illustrated in Fig. 1. Both frames have columns 8.0 in. long and span 12.0 in. long, width 0.750 in. and thickness H about 0.123 in. (steel) and about 0.092 in. (titanium). The frame of type (a) enabled a concentrated impulse to be applied as indicated in Fig. 1(a) to a steel block 0.75 in. by 1.5 in. attached at the midpoint of the span. The frame type (b) had a uniform beam member, as in Fig. 1(b). The feet of the column members were fixed in slots in a steel block of 3 in. depth, as shown, so as to provide clamped end conditions. Corners of the frames are shown in sketches of Fig. 2 to indicate the fabrication techniques. The steel frames used a silver soldered joint with a square brass piece for reinforcement. The corners of the titanium frames were joined by welding, using titanium as the weld metal.

Explosive loading was applied by detonating sheet explosive (Dupont Deta-sheet C) of nominal thickness 0.08 in. To obtain different impulse magnitudes in the concentrated impulse tests, varying numbers of layers of explosive sheet were fixed to the central 3/4 in. square area of the attached block over a 1/4 in. thick pad of Neoprene of the same area. In the distributed impulse tests, strips of explosive sheet of various widths extended over the length of the beam member over buffer strips of 1/8 in. Neoprene. The buffer pads act to reduce peak pressures and reduce local damage. The mass of the pads was very small compared to either the central mass or the mass of the beam so the effect of their inertia was insignificant.

In each test the total impulse applied was measured by the ballistic pendulum device[3] sketched in Fig. 3, the specimen base being bolted on one end of the suspended I-beam. The impulse on the specimen is transmitted through its supporting frame to the pendulum mass. The pendulum mass is large compared to that of the specimen, and its natural period is long compared to the duration of the specimen response or of the pressure pulse. Very accurately,

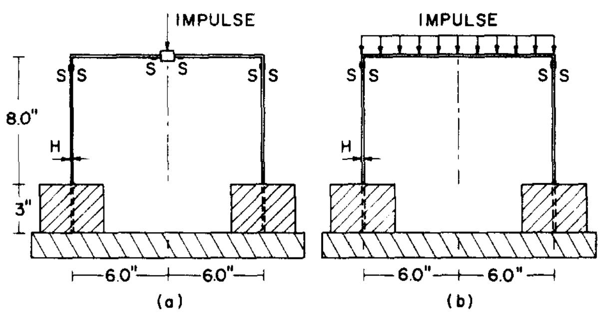

Fig. 1. Types of frame and loading.

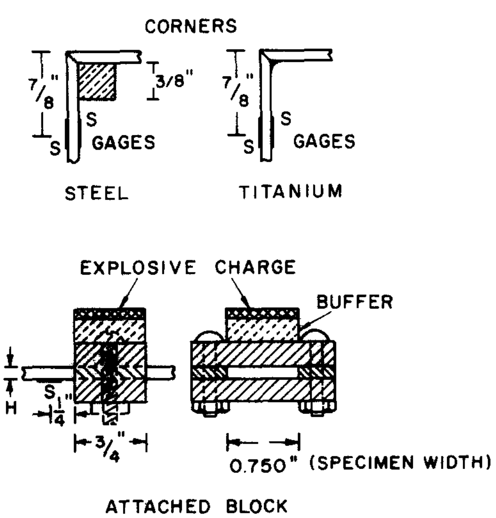

Fig. 2. Details of specimen corners and attached block.

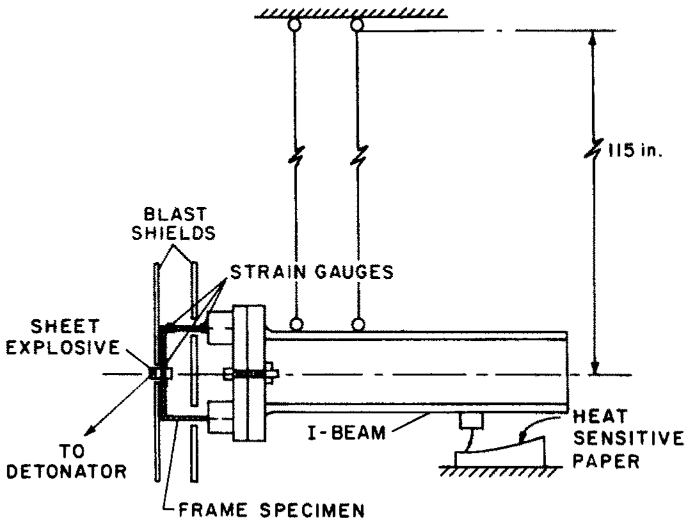

Fig. 3. Test arrangement showing pendulum for impulse measurement.

the impulse I is obtained from the maximum displacement X_m of the pendulum at its mass center by

$$I = \frac{W}{g}\frac{2\pi}{T}X_m \tag{1}$$

where W is the total weight of the pendulum (about 75.8 lb) and T is its natural period (about 3.3 sec).

The impulse calculated from eqn (1) is the correct total impulse on the specimen frame provided the pendulum is acted on only by forces transmitted through the designated loading area of the specimen. Shielding is necessary to prevent extraneous impulsive pressures from reaching the pendulum directly or acting on other areas of the specimen. The main shield was a 1/4 in. steel plate as illustrated in Fig. 2 for the tests with concentrated impulse; for each type of test an aperture fitted closely the loaded area of the specimen. A second shield of 3/4 in. plywood also was inserted since the first shield cannot provide a complete seal. The impulse on the specimen depends not only on the charge weight but on its geometry and on the configuration adjacent to the loaded area; it may also depend on details of the specimen [4]. We measured the impulse in each test instead of relying on calibration factors, keeping a plot of impulse vs charge weight as a rough check.

Information on the time history of the frame response was obtained from wire resistance strain gages. These were SR-4 gages of 1/4 gage length (type FAE-25-12S6) placed at the tops of the columns on both sides, with locations as shown in Figs. 1 and 2. In the tests with concentrated impulse, gages were also placed on the back side of the beam member at distances ranging from 1/8 to 3/8 in. from the attached block as indicated in Fig. 2. We tried to put gages on the beam member in the distributed impulse tests, but these all failed as a result of strong thickness wave effects in these tests. Typical strain records are shown in Fig. 3. Apart from given strain and strain rate data, two response times were obtained from these records, namely time t_f' to reach the first maximum, and the time t_f'' at which the rising signal intersects a line drawn at the final strain magitude. Neither of these directly corresponds to the response time calculated in the mode approximation technique, where rigid-viscoplastic behavior is assumed, but they are of interest for comparison.

3. MATERIAL PROPERTIES

The mild steel specimens were made from hot rolled carbon steel (C1008) supplied as strips 1 in. by 1/8 in. by 10 ft long. They were used without further heat treatment, being milled to width 0.750 in. before fabricating the frames. The thickness as supplied showed negligible variation from the average H = 0.123 in. The titanium frames were made from commercially pure (99.2%) titanium (Ti-50A), supplied as a sheet of 4 ft width. To make the frames, strips 0.750 in. wide were cut in the longitudinal (rolling) direction, and tensile properties measured in this direction were used in the analyses. The thickness H varied by about 1% above and below the average 0.0918 in.

The estimation techniques treat the material as viscoplastic, with behavior in the plastic range that can be described adequately by an equation of the following form:

$$\frac{\sigma}{\sigma_0} = 1 + \left(\frac{\dot{\epsilon}}{\dot{\epsilon}_0}\right)^{1/n} \tag{2}$$

where σ and $\dot{\epsilon}$ are stress and corresponding plastic strain rate, respectively, and σ_0, $\dot{\epsilon}_0$ and n are material parameters of strain rate sensitivity. σ is generally taken as the stress at a specified plastic strain level in test at constant strain rate; however for mild steel we have taken σ as the lower yield stress. The constants σ_0, $\dot{\epsilon}_0$ and n correspond to this choice. Equation (2) generally provides an excellent fit in a least squares sense for strongly rate dependent metals[5]. (However, it should be noted that strain rate history effects are disregarded in this representation.)

Ideally, we should have made tensile stress–strain tests on our materials at strain rates from quasi-static to magnitudes exceeding those in the tested frames; the maximum strain rates in the tests were probably about 50 sec^{-1} so tests to at least 100 sec^{-1} would have been desirable. To avoid the expense of tests at high strain rates we made tests with a conventional testing machine (Instron) at four strain rates from 10^{-4} to 0.1 sec^{-1}. From each of these tests we computed a value of σ_0, using $\dot{\epsilon}_0$ and n values determined from published data on similar metals. Thus we took $\dot{\epsilon}_0 = 40\,\text{sec}^{-1}$, $n = 5$ for mild steel[6, 7] and $\dot{\epsilon}_0 = 120\,\text{sec}^{-1}$, $n = 9$ for titanium[8]. The determination of these constants is discussed in[5]. Typical stress–strain curves are shown in Figs. 5 and 6. If the assumed values of $\dot{\epsilon}_0$, n are valid for our materials, the measured values of σ_0 would be constant. This was found to be the case for mild steel; the four strain rate tests on coupons from any one 10 ft bar furnished an average σ_0 with small scatter and negligible trend with strain rate. For nine bars from which tested frames were fabricated, σ_0 varied from 32.0 to 33.8 ksi; the average value 33.1 ksi was used in the calculations. For our titanium, the four strain rate tests on longitudinal coupons gave σ_0 values which increased slightly with strain rate, indicating that the assumed values of $\dot{\epsilon}_0$ and n were less suitable. However, the r.m.s. deviation from the average 35.2 ksi (at 1% plastic strain) was only about 3%. Strain hardening was larger for this material, and was accounted for approximately in the estimation techniques by repeating the calculation using $\sigma_0 = 37.7$ ksi, corresponding to measured stresses at 2% plastic strain. Numerical values are summarized in Table 1.

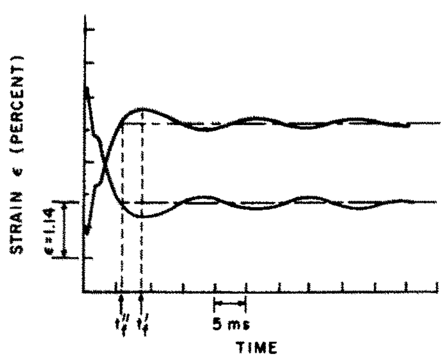

STRAIN GAGES AT TOP OF COLUMN

TEST 12 STEEL FRAME

CONCENTRATED IMPULSE

Fig. 4. Typical strain-time traces.

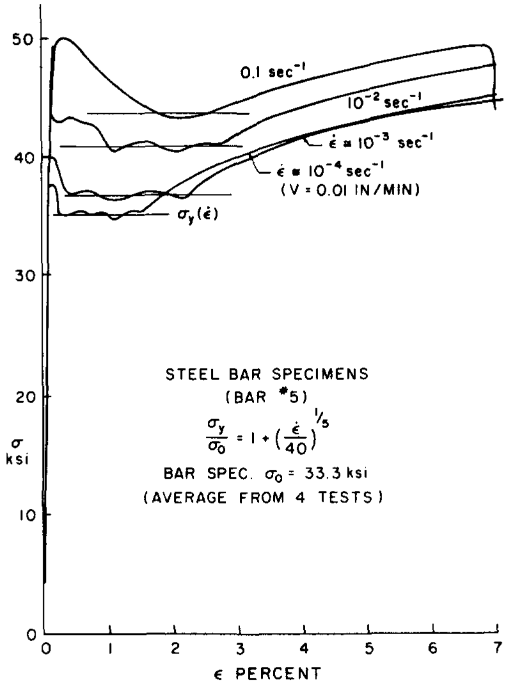

Fig. 5. Typical stress–strain–strain rate records for steel.

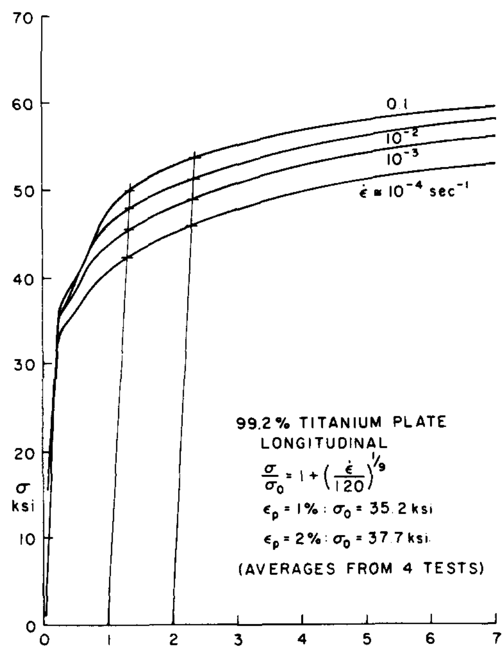

Fig. 6. Typical stress–strain–strain rate records for titanium.

4. TEST RESULTS

Examples of final deflected shapes are shown in Figs. 7–10 for the two types of loading and the two materials; these are typical of large deflection results, with maximum displacement on the order of a third of the span dimension. The curves were traced from the deformed frame before removal from the support base.

The main deflection is that of the midpoint of the beam member, labelled w_c^f, and shown in Figs. 11, 12, 14 and 15 as a function of the impulse I. A secondary deflection magnitude is the

Table 1.

		Steel Frames	Titanium Frames
Strain rate constant[1]	σ_o psi	33,100[2]	35,200[3] at $\varepsilon^p = 1\%$ 37,700[3] at $\varepsilon^p = 2\%$
Strain rate constant[1]	$\dot{\varepsilon}_o$ sec^{-1}	40	120
Strain rate constant[1]	n	5	9
Mass density	ρ lb $sec^2 in.^{-4}$	0.73×10^{-3}	0.42×10^{-3}
Total span type (a)	$2L_1 + 2a$ in.	12.00	12.00
type (b)	$2L_1$ in.	12.00	12.00
Width of attached block (type (a) frame)	2a in.	0.75	0.75
Column height	L_2 in.	8.00	8.00
Thickness	H in.	0.123	0.092
Width	b in.	0.750	0.750
Attached block weight (including enclosed beam section)	G lb	0.21	0.21

[1]As used in Eq. (2).
[2]Lower yield stress; average for nine bars, from four strain rates for each bar.
[3]Longitudinal (rolling) direction.

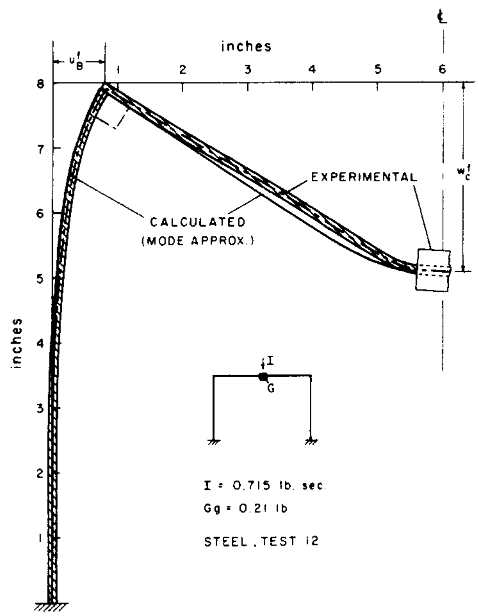

Fig. 7.

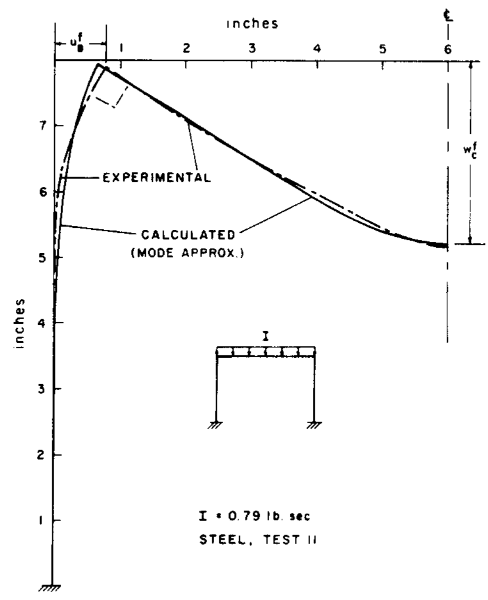

Fig. 8.

Fig. 7. Typical final shape at large deflection—steel.

Fig. 8. Typical final shape at large deflection—steel.

inward motion of the corner, marked u_B^f in Figs. 7–10. This is shown in Figs. 13 and 16 as function of I. The quantity plotted is the average for the two corners, the deformation being slightly unsymmetric in some cases. The test data are summarized in Table 2.

In Figs. 17 and 18 are shown the measured response times t_f' and t_p'' plotted vs impulse. As illustrated in Fig. 4, t_f' is the peak response time and t_f'' is the time at which the final strain magnitude is first reached; i.e. it is the intercept of a line drawn at the final strain level with the rising strain signal. In the tests on titanium frames, strain records were obtained mainly from

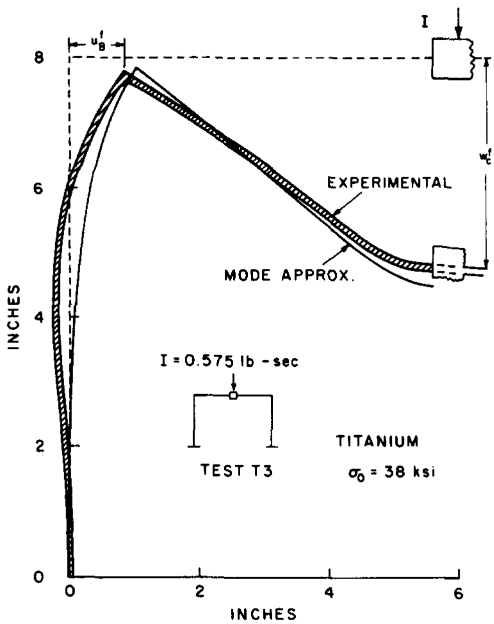

Fig. 9. Typical final shape at large deflection—titanium.

Table 2.

Test No.	Bar No.	Thickness H in.	σ_0 ksi	Charge Weight Grams	Impulse lb-sec	Final Deflection at Center w_c^f in.	Final Deflection Top of Column u_B^f in.	Time to Reach Max. Strain t_f' msec.	Intercept Time t'' msec
STEEL FRAMES									
Concentrated Impulse									
S2	5	0.123	33.3	2.1	0.542	1.70	0.31	7.0	4.5
S3	5	0.123	33.3	2.6	0.61	2.03	0.430	7.8	5.4
S5	4	0.123	32.0	1.3	0.303	0.52	0.047	4.0	2.0
S6	8	0.123	33.8	1.6	0.40	0.83	0.094	5.0	3.0
S8	6	0.123	33.5	4.2	0.75	3.52	1.18	10.0	6.4
S9	6	0.123	33.5	3.7	0.71	3.06	0.89	9.0	-
S12	9	0.123	33.4	3.4	0.715	2.90	0.84	9.0	6.0
S13	3	0.123	33.15	2.8	0.66	2.59	0.68	-	-
Uniform Impulse									
S10	7	0.123	33.1	2.4	0.505	1.125	0.15	4.0	2.0
S11	7	0.123	33.1	3.65	0.79	2.83	0.78	6.5	4.2
S14	9	0.123	33.4	3.1	0.70	2.23	0.49	-	-
TITANIUM FRAMES									
Concentrated Impulse									
T1		0.0911	35.0*	1.16	0.34	0.6	0.03	6	
T2		0.0913	35.0	2.1	0.56	3.09	0.92	8	2 (?)
T3		0.0928	35.0	2.2	0.575	3.25	0.94	8	2 (?)
T4		0.0927	35.0	1.65	0.492	2.03	0.41	7	2 (?)
T5		0.0902	35.0	2.6	0.66	5.12	2.34	8.5	3 (?)
T9		0.0925	35.0	1.4	0.47	1.83	0.33	7	2 (?)
T12			35.0	1.2	0.355	0.68	0.03	6.5	2 (?)
Uniform Impulse									
T6		0.0905	35.0	2.6	0.623	7.56	4.42		
T7		0.0914	35.0	1.4	0.323	1.34	0.20		
T8		0.0920	35.0	2.0	0.466	3.34	0.95		
T11		0.0894	35.0	1.7	0.336	1.80	0.34		

*At 1 percent strain; for 2 percent strain σ_0 = 38.0 ksi.

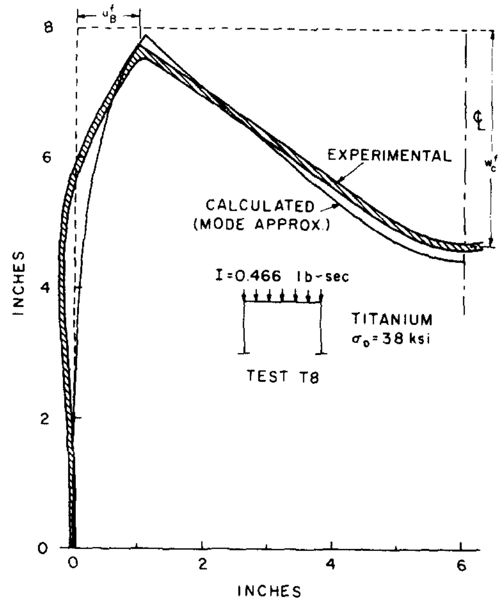

Fig. 10. Typical final shape at large deflection—titanium.

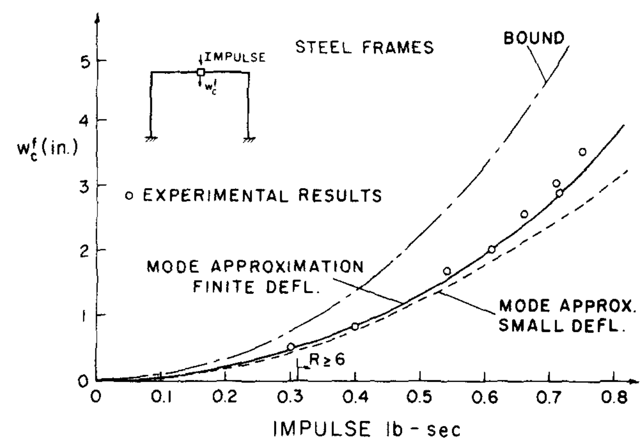

Fig. 11. Final transverse deflection vs impulse, steel frames.

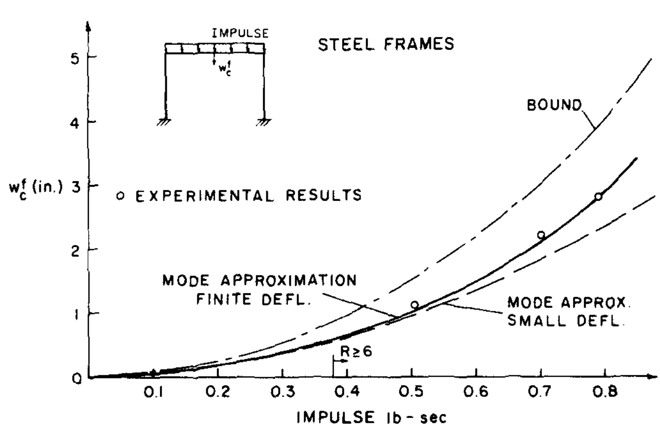

Fig. 12. Final transverse deflection vs impulse, steel frames.

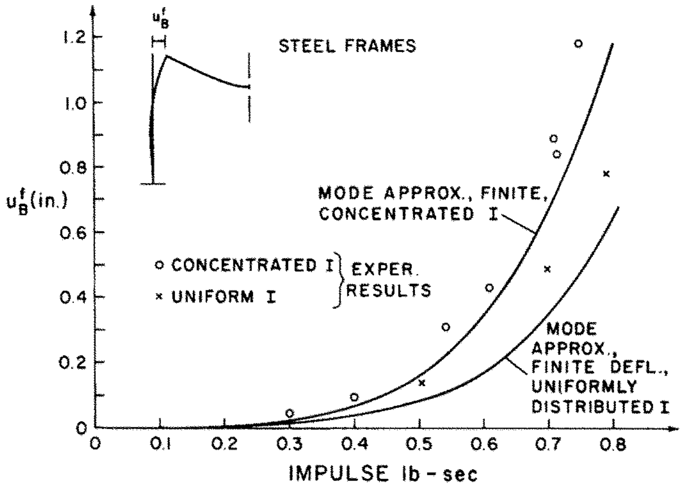

Fig. 13. Final inward deflection at corner vs impulse.

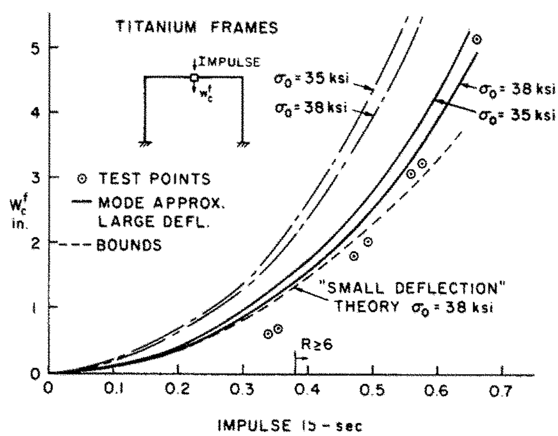

Fig. 14. Final transverse deflection vs impulse, titanium frames.

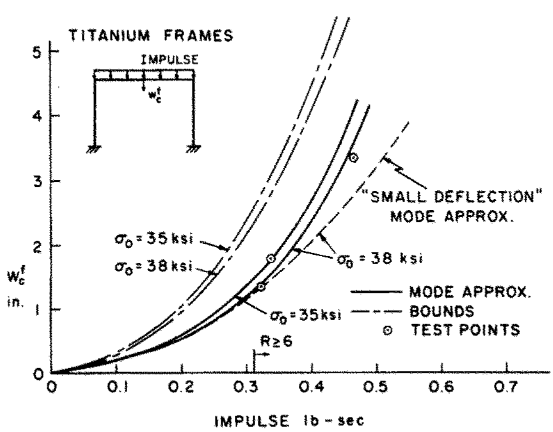

Fig. 15. Final transverse deflection vs impulse, titanium frames.

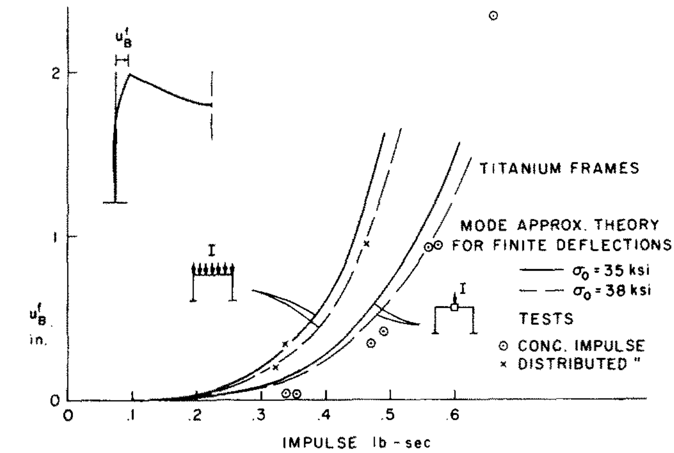

Fig. 16. Final inward deflection at corner vs impulse.

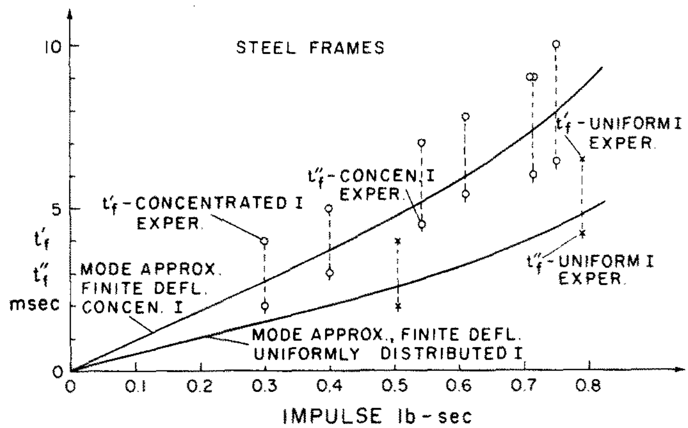

Fig. 17. Response times vs impulse.

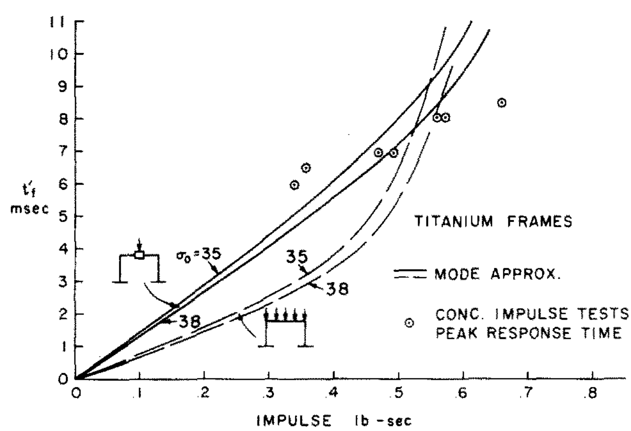

Fig. 18. Response times vs impulse.

gages at the tops of the columns. At these locations the plastic strain is relatively small, and the record does not furnish the intercept time t_f'' accurately. Hence in Fig. 18 test results are shown only for the peak response time t_f' for the concentrated mass tests. The gage records showed a plateau rather than a distinct peak; t_f' was taken as the time when this was first reached. For the tests with uniform impulse, meaningful determination of either time did not seem possible, probably because of strong elastic effects.

The most informative strain gage records were obtained for the steel frames with central mass. In these tests, the gages near the top of the columns registered strain rates of 5–10 sec^{-1} and permanent strains of 0.5–1.2% over the range of impulse values. The response of gages attached near the central mass depended critically on the exact location of the gage since the plastic straining was very localized. For test number 12 shown in Fig. 7 ($I = 0.715$ lb sec) a strain gage placed 1/8 in. away from the edge of the central mass indicated a strain rate of 30 sec^{-1} and a permanent strain of about 3%. These seem to be close to the maximum strain rates and strains experienced by the frame specimens in these tests.

5. DISCUSSION

We are interested in comparing the measured deflections with upper bounds on the deflections, and the test deflections and response times with the approximate final deflections and durations obtained from the mode approximation technique. Details on this technique appear in a companion paper[1]. Here we compare the test results with those of the estimation techniques with particular attention to indications concerning the errors in the two approaches.

As already noted, we can distinguish between intrinsic errors and those due to further approximations and idealizations. In the bound approach, the intrinsic error arises from the substitution of a problem of static equilibrium for the original dynamic one; use of the theorem of minimum potential energy makes the intrinsic error positive, i.e. furnishes an upper bound. In the mode approach, the intrinsic error arises from the technique used to determine the magnitude of the initial mode velocity field from the initial velocity field. This gives the relation between the initial mode velocity amplitude $\dot{w}_c^*$ and prescribed initial velocity $\dot{w}_c^0$; their ratio is less than one for the concentrated impulse and greater than one for the uniformly distributed impulse. Thus the intrinsic error of the mode method is negative (underestimates deflections) in the first case and positive (overestimates deflections) in the second.

If all the conditions underlying the estimation techniques were exactly satisfied, the comparison with test results would show the intrinsic error only. Figures 11 and 12 for steel frames would show test points above and below, respectively, the curve for the mode approximation (for finite deflections). Similarly Figs. 14 and 15 for titanium frames would show the test points above and below, respectively, the mode approximation curve. The actual test results do not show these relations consistently. Figures 11 and 12 do seem to be in fair agreement with expectations based on the intrinsic error, since in Fig. 11 the test deflections lie slightly above the estimated curve, and in Fig. 12 they are essentially on it. However, Figs. 14 and 15 (for titanium frames) show the opposite relations. For concentrated loading the observed deflections are too small, while for the distributed impulse tests they are only slightly below or on the curve for $\sigma_0 = 35$ ksi, and on or above the curve for $\sigma_0 = 38$ ksi. The two estimation curves are drawn in these figures as a way of taking rough account of strain hardening, which is more pronounced in titanium than in steel; the two values correspond to plastic strain 1% and 2%, respectively, in the determination of σ_0 from the strain rate tests. Agreement is better if $\sigma_0 = 38$ ksi is used, but the relation of test to estimated deflections remains opposite to what would occur if the intrinsic error dominated.

Explanations for this behavior must be sought by considering other errors in the application of the mode technique than the intrinsic error so far considered. For this calculation (and for the deflection bound as well) a number of idealizations were made, particularly with respect to material behavior. These are listed below:

(1) Elastic deformations were neglected.

(2) Plastic strain rates were written as explicit functions of stresses, with implicit consideration of strain hardening.

(3) Strain rate history effects were neglected.

(4) A homogeneous viscous stress–strain rate representation (without yield condition) was used in place of a homogeneous viscoplastic law, making use of matching technique[5, 9].

(5) Essentially flexural behavior was assumed, the center-line strain being assumed zero, and axial forces disregarded in the constitutive equations (treated as reactions).

(6) The pressure pulse was idealized as impulsive, i.e. as a finite impulse with zero duration.

(7) In the extended mode technique, "instantaneous" mode form solutions were found

appropriate to the current deflection field, and a succession of such solutions was made continuous only with respect to the major deflection.

(8) The numerical determination of the static solution in the bound method and of mode form solutions in the mode technique was carried out by iterative schemes.

Arguments can be made [1] that almost all of the idealizations or approximations listed above lead to positive errors, i.e. to estimated deflections exceeding the actual ones. The neglect of axial forces in the yield condition, item (5), may be an exception; assuming center-line axial strain zero is equivalent to assuming a stronger structure than the actual one. However it is not clear whether requiring the deformation to be absorbed entirely by flexural deformations should lead to larger or smaller magnitudes of the major deflection. The constraints are not ones that require center-line strains to occur even at very large deflections. This idealization was believed to cause negligible error, but no direct check of this is available. Similarly, the numerical determination of instantaneous mode form solutions by iterative schemes is believed very accurate in the present cases, since convergence was rapid throughout. The neglect of plastic strain rate history is believed to cause a positive error, but the experimental evidence (mainly from tests in which the strain rate is rapidly increased) is very slight.

The influence of elastic deformations, neglected in the constitutive equations used, is difficult to assess. A rule-of-thumb energy criterion for validity of this neglect is a large value of the ratio of input energy to a measure of the elastic strain energy capacity of the structure. If this ratio R is greater than about 6 in a simple one-degree-of-freedom model, the neglect of elastic effects causes a positive error of about 15%. If this holds in the present frame structures, the impulse should exceed about 0.45 lb-sec in the tests with concentrated impulse and about 0.25 lb-sec in those with distributed impulse; the required impulse is marked on Figs. 11, 12, 14 and 15. The importance of elastic effects as indicated by this energy criterion appears essentially the same for both the steel and the titanium frames. The tests on titanium frames with concentrated impulse in Fig. 14 do show exactly the relation to the estimated deflection curves (for large displacements) that one would expect if the main discrepancies are due to the neglect of elastic deformations. The steel frames under concentrated impulse (Figs. 11) show similar trends, but the test points fall on the estimated deflection curve at small impulse magnitudes, and lie above it at higher impulses (rather than approaching the calculated curve from below).

The measurements of final inward displacement at the two corners (averaged for each frame) are shown in Fig. 13 (steel) and Fig. 16 (titanium). Comparison of these secondary deflection magnitudes with those predicted by the extended mode technique is of interest because this deflection is zero according to the mode technique for small deflections. The mode technique predicts these deflections reasonably well at the larger impulse values.

A possible "experimental" error, which could cause the steel test frames to deflect more than expected, is a weakening at the corners where the beam member is silver-soldered to the two columns. This seems unlikely, however, since silver soldering requires fairly low temperatures, and the joints are strengthened by brass blocks as shown in Fig. 2. Moreover, static tests [10] on steel frames fabricated in the same way failed to show weaker behavior, when loads at first yield, first hinge development, and plastic collapse were compared with the calculated loads using yield stress measured at strain rates approximating those of the frame tests (about 10^{-3} sec^{-1}). This explanation also must be rejected.

In conclusion, it can be said that the deflection upper bounds are verified by the tests, and that the extended mode approximation method leads to deflection estimates close to those observed in the tests on steel frames, and below or close to those measured in the tests on titanium frames. Corroboration was not obtained of the intrinsic error of the mode technique, and further investigation of the various additional sources of error is required. However, the closeness of predicted to test results suggests that practical use of the approximation techniques can be made before such investigations are completed.

Acknowledgements—Mr. George LaBonte, Technical Assistant, gave invaluable assistance with the explosive tests and the strain gage measurements. Mr. Duty Mowry, Technical Assistant, expertly fabricated the frames. Mr. Michael Chosak, Research Engineer, was helpful in connection with tests on material behavior. We express our appreciation to them, and we also thank Prof. R. J. Clifton and the National Science Foundation for making available funds from NSF Grant ENG75-01426 which enabled the test program on titanium frames to be completed. All staff mentioned are at Brown University.

REFERENCES

1. P. S. Symonds and C. T. Chon, Large viscoplastic deflections of impulsively loaded plane frames. *Int. J. Solids Structures* **15**, 15–31 (1978).
2. S. R. Bodner and P. S. Symonds, Experiments on Viscoplastic Response of Circular Plates to Impulsive Loading. Technical Report of Brown University under Grant NSF 74-21258 and Contract N00014-75-C-0860.
3. S. R. Bodner, Deformation of rate sensitive structures under impulsive loading. In *Engineering Plasticity* (Edited by J. Heyman and F. A. Leckie), pp. 77–91. Cambridge University Press (1968).
4. T. A. Duffey and S. W. Key, Experimental-Theoretical Correlations of Impulsively Loaded Clamped Circular Plates. *Res. Rep. SC-RR*-68-210, Sandia Laboratories (April 1968).
5. P. S. Symonds and C. T. Chon, Approximation Techniques for Impulsive Loading of Structures of Time-Dependent Plastic Behavior With Finite Deflections. *Proc. Oxford Conf., Mechanical Properties of Materials at High Strain Rates*, Inst. of Physics Conf. Ser. No. 21 (Edited by J. Harding), pp. 299–315 (1974).
6. M. J. Manjoine, Influence of rate of strain and temperature on yield stresses of mild steel. *J. Appl. Mech.* **11**, A211–A-218 (1944).
7. R. J. Aspden and J. D. Campbell, The effect of loading rate on the elasto-plastic flexure of steel beams. *Proc. R. Soc.*, **A290**, 266–285 (1966).
8. J. C. C. Hsu and R. J. Clifton, Plastic waves in a rate sensitive material—I. Waves of uniaxial stress. *J. Mech. Phys. Solids* **22**, 233–253 (1974).
9. P. S. Symonds, Approximation techniques for impulsively loaded structures of rate sensitive plastic behavior. *SIAM J. Appl. Math.* **25**(3) 462–473 (1973).
10. C. T. Chon and P. S. Symonds, Large dynamic deflection of plates by mode methods. *J. Engng Mech. Div., Proc. ASCE* **103**(EM1), 3–14 (1977).
11. E. Exner, M. Mak, P. Moynihan, J. Pappas and D. Wojcieszak, Structural analysis of a clamped portal frame under static point loading. Project Report in Course EN 12, Division of Engineering, Brown University (1976).